JOURNAL OF MATERIALS SCIENCE 26 (1991) 3032–3040

# Mechanical properties of the $Ni_3(Si, Ti)$ alloys doped with carbon and beryllium

TAKAYUKI TAKASUGI
*Institute for Materials Research, Tohoku University, Sendai, 980 Japan*
MITSUHIKO YOSHIDA
*Miyagi National College of Technology, Natori, Miyagi-prefecture, 981-12 Japan*

The $Ni_3(Si, Ti)$ alloys doped with small amounts of carbon and beryllium were tensile tested in two environments, vacuum and air, over a wide range of test temperatures. The yield stresses of the carbon-doped alloys were almost identical to the undoped alloys while those of the beryllium-doped alloys were slightly higher than the undoped $Ni_3(Si, Ti)$ alloys. The doping with carbon enhanced the elongation and ultimate tensile strength (UTS) whereas doping with beryllium reduced the elongation over the entire temperature range tested. The fracture patterns were primarily associated with the ductility behaviour. As the elongation (or UTS) increased, the fracture pattern changed from the intergranular to the transgranular fracture patterns. No environmental embrittlement of the ductility of the carbon-doped alloys was found at ambient temperatures but it was evident at elevated temperatures. Ductilities were reduced at high temperatures when the carbon-doped alloys were tensile tested in air. At high temperatures the environmental embrittlement observed is suggested to be due to the penetration of (free) oxygen into the grain boundaries causing the ductility loss in the carbon-doped alloys.

## 1. Introduction

It is expected that $Ni_3Si$ intermetallic alloys with $L1_2$ structure will offer potential applications to high-temperature structural materials and chemical parts, because of their high strength and good chemical stability. It was found recently that $Ni_3Si$ alloyed with $\sim$ 3.2 at % Ti displayed some ductility at room temperature [1]. This ductilization was consistent with the alloying method used to improve the grain-boundary cohesion of $L1_2$-type ordered alloys proposed previously [2, 3]. Based on the careful control of the content of the additive atoms Ti and the alloy stoichiometry, it was demonstrated that $Ni_3Si$ alloys in the as-cast [4] and in recrystallized [5, 6] forms were ductilized and also strengthened over a wide range of test temperatures; the yield strength increased with increasing Ti content and with decreasing Ni content at all test temperatures, while the elongation at room temperature increased with both increasing Ti content and Ni content [4].

To improve further the mechanical properties of the $Ni_3(Si, Ti)$ alloys, the quaternary $Ni_3(Si, Ti)$ alloyed with additions of substitutional elements (Hf, Nb, Cr, Mn and Fe) were studied in their polycrystalline forms [7]. On the other hand, it is known that an interstitial atom has a significant effect on the mechanical properties of the $L1_2$-type ordered alloys through the lattice behaviour in perfect lattices, or at the grain boundaries. In the previous work, the effect of boron in $Ni_3(Si, Ti)$ alloys on the lattice properties, solubility [8], and also on mechanical properties [4–6] has been investigated. It was observed that the boron behaved as an interstitial atom in $Ni_3(Si, Ti)$ alloys and produced a higher elongation value than the undoped $Ni_3(Si, Ti)$ alloys over a wide range of test temperatures [4–6]. It was also shown, by tensile tests in different test environments (air and vacuum), that the addition of boron suppressed hydrogen embrittlement at ambient temperatures but, on the other hand, caused oxygen embrittlement at high temperatures [6]. Whether a similar effect is shown by additions of different kinds of small-diameter atoms, i.e. carbon and beryllium, is very interesting.

In the present work, the mechanical properties of yield stress, ultimate tensile stress (UTS), elongation and fracture of the $Ni_3(Si, Ti)$ alloys doped with carbon and beryllium, were investigated. The main objectives were to understand the effect of the dopants, the test temperature and the test environment on these properties. The mechanical properties characterized by fractographic observation, were correlated with the microstructural feature and then compared with those obtained for undoped $Ni_3(Si, Ti)$ alloys and also alloys doped with boron [5, 6], whose compositions were exactly the same as the present alloys.

## 2. Experimental procedure

The base composition used in this work was 79.5 at % Ni, 11 at % Si and 9.5 at % Ti and located in a single-phase region of the $L1_2$ structure as shown in Fig. 1


0022–2461/91 $03.00 + .12 

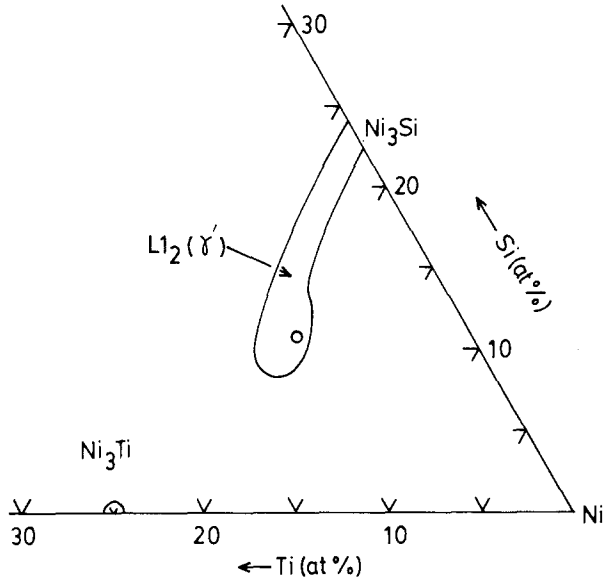


*Figure 1* (○) Chemical composition of the $Ni_3(Si, Ti)$ alloys used, located in a phase field of $L1_2$ structure.

[8]. This composition was identical to those of the undoped and boron-doped $Ni_3(Si, Ti)$ alloys previously studied [5, 6]. Alloys with this composition were prepared by nonconsumable arc melting in an argon atmosphere. Nickel (99.9 wt % purity), silicon (99.999 wt % purity) and titanium (99.8 wt % purity) were used as starting materials. The carbon was doped using a master alloy of Ti–7.4 wt % carbon which was pre-alloyed from the carbide of TiC and pure titanium, while the beryllium was directly doped using the pure metal. The nominal and analysed chemical compositions of the alloys used in this work are shown in Table I; the agreement between the two values is fairly good.

Alloy buttons of dimensions approximately 15 mm × 15 mm × 80 mm, were prepared and then homogenized at 1323 K for 1 day in vacuum. These buttons were worked to plates of about 1 mm thickness by repeatedly rolling (at 573 K in air) and annealing (at 1273 K in vacuum). The annealing for recrystallization was done at 1273 K for 5 h in vacuum.

After heat treatment, metallographic examination, X-ray analysis and transmission electron microscopic (TEM) observation were performed to characterize the microstructures of these alloys. The metallographic observation was done on plate specimens which were electrolytically polished in a solution of 15% $H_2SO_4$ and 85% $CH_3OH$ and then etched in a marble solution. X-ray diffraction measurements were also performed on plate specimens, using $CuK_\alpha$ radiation. Higher index lines of (2 2 0) were used to determine the lattice parameter. Thin foil specimens for TEM observation were prepared by electropolishing in a solution of 20% $H_2SO_4$ and 80% $CH_3OH$ at 273 K. The thin foil specimens were then examined in a JEM 100B operated at 100 kV and also a JEM 2000FX operated at 200 kV, equipped with an energy dispersive X-ray spectrometer (EDX).

The tensile specimens of dimensions 1.2 mm × 2.2 mm × 14 mm gauge length were prepared by a precision wheel cutter and an electro-erosion machine. The faces of the specimens were abraded on SiC paper. The tensile tests were carried out using an Instron testing machine at a nominal strain rate of $1.2 \times 10^{-3}\ s^{-1}$. The testing temperatures were from 77–1073 K. The tests at 77 K were performed in a Dewar vessel filled with liquid nitrogen. The tensile tests at room temperature and at elevated temperatures were conducted in environmental atmospheres of air or vacuum (better than $1.3 \times 10^{-3}$ Pa). After tensile testing, the fracture surfaces of the specimens were examined by a scanning electron microscopy (SEM).

## 3. Results

### 3.1. Microstructure

Fig. 2 shows the optical microstructures of the carbon (0.06 wt %)-doped (Fig. 2a) and beryllium (0.1 wt %)-doped (Fig. 2b) $Ni_3(Si, Ti)$ alloys. The former alloy exhibited a number of second-phase particles and had an average grain size of about 31 μm. The $Ni_3(Si, Ti)$ alloys doped with 0.03 wt % carbon also exhibited second-phase particles. Thus, it appears that the solubility limit of carbon in $Ni_3(Si, Ti)$ alloy is extremely low, i.e. less than 0.03 wt % (~0.2 at %). On the other hand, the beryllium-doped alloy exhibited, apparently, a single-phase structure with average grain size about 40 μm. Thus, the solubility limit of beryllium in the $Ni_3(Si, Ti)$ alloy was larger than those of carbon and boron (i.e. below 50 p.p.m. (~0.03 at %) [8]), that is, more than 0.1 wt % (0.5 at %).

Figs 3 and 4 show the TEM bright-field images of both alloys. The carbon-doped $Ni_3(Si, Ti)$ alloy showed cuboidal second phases in the grain interior which appear to be incoherent with the matrix (Fig. 3a). Chemical analysis by EDX indicated that these particles were titanium carbide (probably TiC) and contained neither of the constituent elements, silicon or nickel. The grain boundaries in this alloy contained no second phases and were relatively straight, as seen in Fig. 3b. On the other hand, the beryllium-doped

TABLE I Chemical compositions of the $Ni_3(Si, Ti)$ alloys used in this work

| Alloy | Nominal (analysed) composition | | | | |
|---|---|---|---|---|---|
| | Ni (at %) | Si (at %) | Ti (at %) | Carbon (wt %) | Beryllium |
| $Ni_3(Si, Ti)$ + 0.03C | 79.5(–) | 11(10.58) | 9.5(9.54) | 0.03(0.028) | |
| $Ni_3(Si, Ti)$ + 0.06C | 79.5(–) | 11(10.58) | 9.5(9.51) | 0.06(0.062) | |
| $Ni_3(Si, Ti)$ + 0.1Be | 79.5(–) | 11(10.66) | 9.5(9.55) | | 0.1(0.102) |

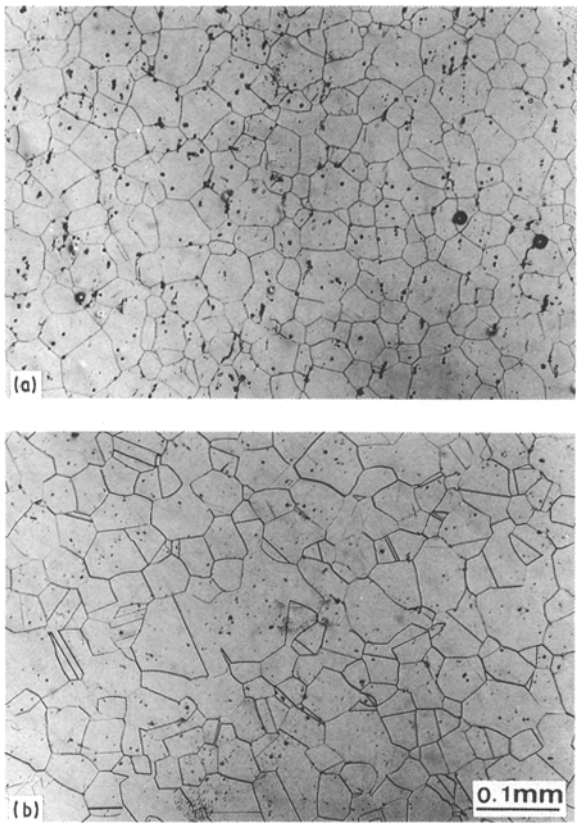


*Figure 2* Optical microstructures of (a) the carbon (0.06 wt %)-doped and (b) the beryllium (0.1 wt %)-doped $Ni_3(Si, Ti)$ alloys.

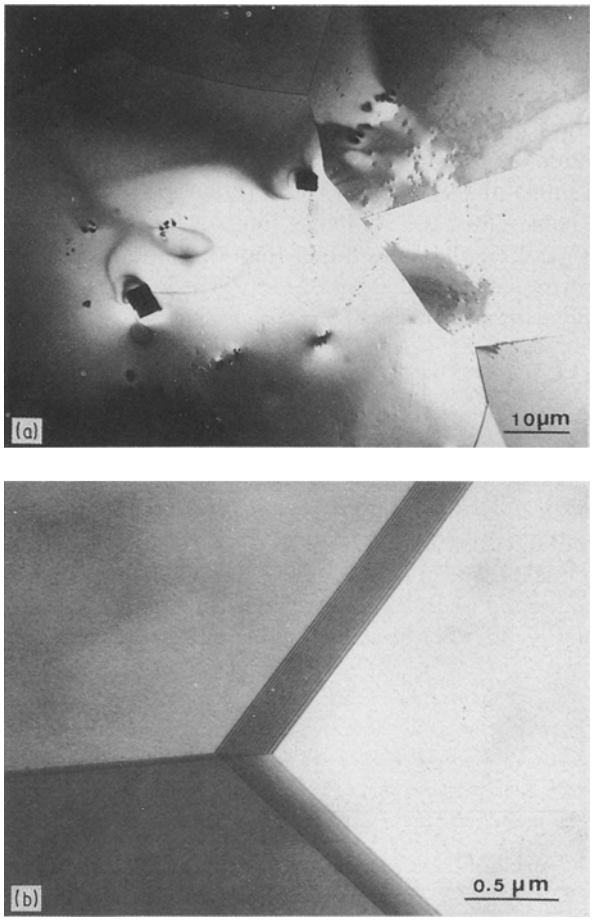


*Figure 3* TEM bright-field images for the carbon (0.06 wt %)-doped $Ni_3(Si, Ti)$ alloy.

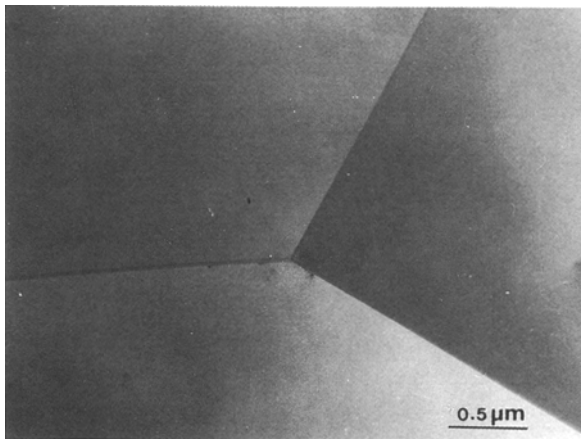


*Figure 4* TEM bright-field image for the beryllium (0.1 wt %)-doped $Ni_3(Si, Ti)$ alloy.

$Ni_3(Si, Ti)$ alloy exhibited a single-phase structure not only in the grain interior but also at the grain boundaries as shown in Fig. 4.

The measured lattice parameters were shown to be 0.355 06 nm for the carbon-doped $Ni_3(Si, Ti)$ alloys and insensitive to the carbon content. These values are very close to the value of the undoped $Ni_3(Si, Ti)$ alloy, i.e. 0.355 05 nm [8]. This result again reveals that the solubility limit of carbon in this alloy is extremely low. On the other hand, the lattice parameter measured for the beryllium-doped $Ni_3(Si, Ti)$ alloy was 0.354 86 nm, a value which is certainly smaller than that of the undoped $Ni_3(Si, Ti)$ alloy. This result thus suggests that the beryllium behaved as substitutional atoms in this alloy.

## 3.2. Tensile properties

### *3.2.1. Tensile tests in vacuum*

Fig. 5 summarizes the temperature dependence of the yield stress (defined as an offset stress of 0.2% plastic

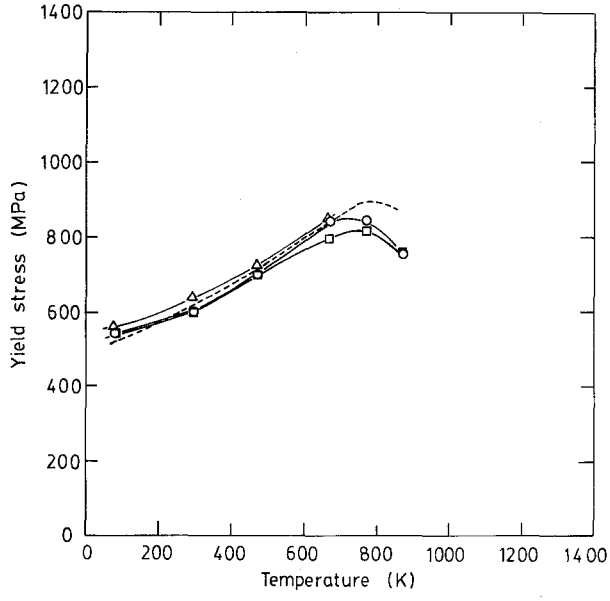


*Figure 5* Variations of the 0.2% yield stress of the carbon-doped $Ni_3(Si, Ti)$ alloys and the beryllium-doped $Ni_3(Si, Ti)$ alloys with test temperature. Note that the tests were performed in vacuum and the data for the undoped $Ni_3(Si, Ti)$ alloys (– – –) are included for comparison. (○) 0.03 wt % C, (□) 0.06 wt % C, (△) 0.1 wt % Be.

strain) of the carbon-doped and beryllium-doped $Ni_3(Si, Ti)$ alloys. These data were taken from the tensile tests under vacuum conditions. In this figure, the data for the undoped $Ni_3(Si, Ti)$ alloys [5] are included for comparison. In all of the alloy systems, the yield stresses began to increase from 77 K with increasing temperature, reached a maximum and then tended to decrease at high temperatures.

The levels of the yield stresses of the carbon-doped $Ni_3(Si, Ti)$ alloys were almost identical to the undoped $Ni_3(Si, Ti)$ alloys at temperatures below the peak [5]. Also, difference in yield stress caused by varying the carbon content was not evident. These results imply that the carbon content in the solution was too low to produce solid solution strengthening and also the volume fraction of second-phase particles was too low to create precipitation strengthening. However, the levels of yield stresses of the carbon-doped $Ni_3(Si, Ti)$ alloys at temperatures above the peak were clearly lower than those of the undoped $Ni_3(Si, Ti)$ alloys [5]. On the other hand, the yield stresses of beryllium-doped $Ni_3(Si, Ti)$ alloys were slightly higher than the undoped $Ni_3(Si, Ti)$ alloys, reflecting the solid solutioning of the beryllium atoms in the solution.

Fig. 6 summarizes the variations of elongation (Fig. 6a) and UTS (Fig. 6b) of the carbon-doped and beryllium-doped $Ni_3(Si, Ti)$ alloys with testing temperature. These data were again taken from the tensile tests under vacuum conditions. In this figure, it is clearly seen that the elongation of the carbon-doped $Ni_3(Si, Ti)$ alloys was consistently higher than that of the undoped $Ni_3(Si, Ti)$ alloys and also displayed almost the same values in the two carbon contents; elongation remained almost constant up to 673 K and then rapidly decreased with increasing temperature. On the other hand, the elongation of the beryllium-doped $Ni_3(Si, Ti)$ alloys was much lower than the undoped $Ni_3(Si, Ti)$ alloys and decreased monotonically from 77 K with increasing temperature.

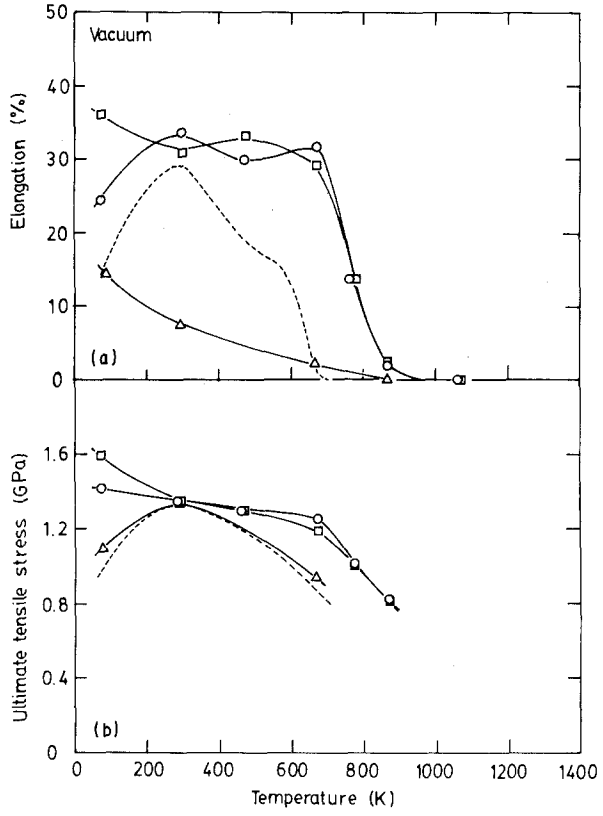


*Figure 6* Variations of (a) elongation and (b) UTS of the carbon-doped $Ni_3(Si, Ti)$ alloys and the beryllium-doped $Ni_3(Si, Ti)$ alloys with test temperature. Note that the tests were performed in vacuum and the data for the undoped $Ni_3(Si, Ti)$ alloys are included for comparison. For key, see Fig. 5.

The UTS behaviour in terms of dopants and test temperature was basically similar to that of elongation; UTS was higher in the carbon-doped $Ni_3(Si, Ti)$ alloys than in the undoped $Ni_3(Si, Ti)$ alloys. However, the UTS of beryllium-doped $Ni_3(Si, Ti)$ alloys was almost identical to that of the undoped $Ni_3(Si, Ti)$ alloys. The UTS of the carbon-doped $Ni_3(Si, Ti)$ alloys decreased monotonically from 77 K with increasing temperature while the UTS of the undoped and beryllium-doped $Ni_3(Si, Ti)$ alloys was the highest at room temperature and decreased from 300 K with increasing temperature.

Fig. 7 shows the variation of the fractographic patterns observed in the carbon (0.06 wt %)-doped $Ni_3(Si, Ti)$ alloys with the test temperature. The transgranular fracture with the dimple-like patterns was dominant at 77 K and at room temperature, and the intergranular fracture patterns tended to be more dominant with increasing temperature. For the beryllium-doped $Ni_3(Si, Ti)$ alloys, the intergranular fracture mode was more dominant than the carbon-doped and undoped $Ni_3(Si, Ti)$ alloys as clearly represented in Fig. 8, where the fracture pattern of the specimen tested at room temperature is shown. Thus, the fracture surfaces of the tensile specimens exhibited a variety of fracture patterns, depending on the testing temperatures and the alloys. However, the fracture patterns were primarily correlated with the degree of the elongation (or the UTS) itself. As the elongation (or the UTS) value increased the fracture pattern changed from the intergranular to the transgranular fracture patterns.

### 3.2.2. Tensile tests in air

The yield stresses obtained from the tensile tests in air were identical to those obtained from tensile tests in vacuum over the whole test temperature range. Thus, it is obvious that the yield stresses in all the alloy systems observed in this work was little affected by the environmental medium.

Figs 9 and 10 illustrate the variations of elongation (Fig. 9a) and UTS (Fig. 10a) with testing temperature for the carbon-doped $Ni_3(Si, Ti)$ alloys. These data were compared between the two environmental media. The data for the boron-doped (Figs 9b and 10b) and the undoped $Ni_3(Si, Ti)$ alloys (Figs 9c and 10c), which have been reported previously [5, 6], are also included in these figures.

For the carbon-doped $Ni_3(Si, Ti)$ alloys, the elongation and UTS values at room temperature were almost the same in the two environmental media. However, as the test temperature increased, the elongation and UTS values of the specimens tested in air decreased more than did those of specimens tested

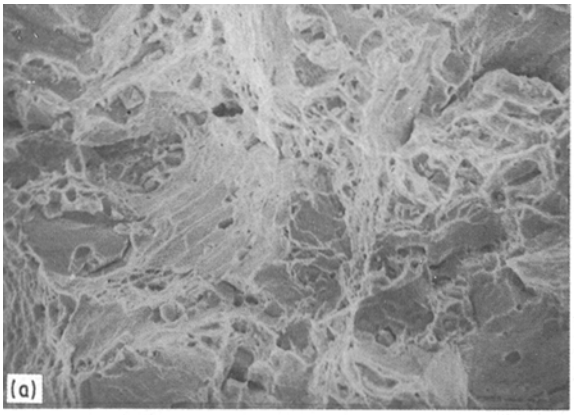


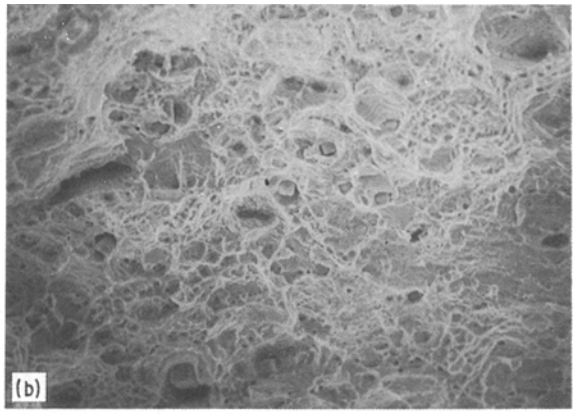


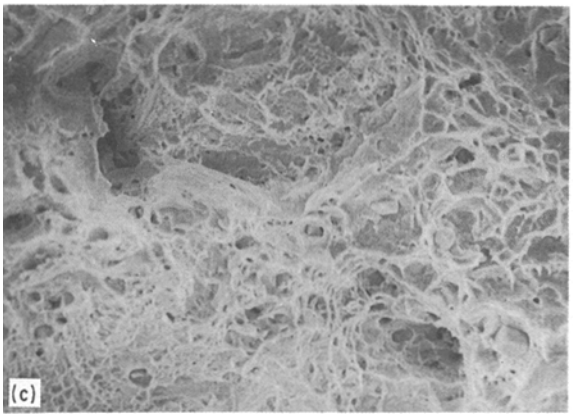


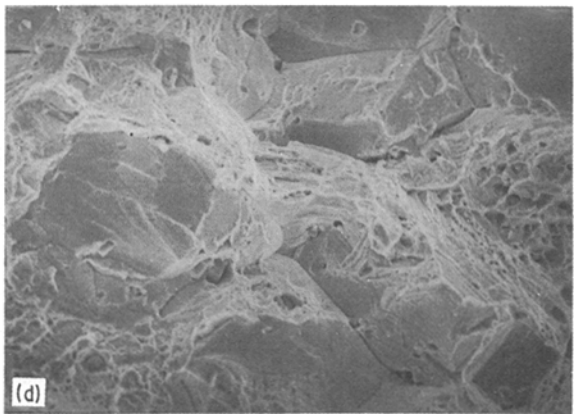


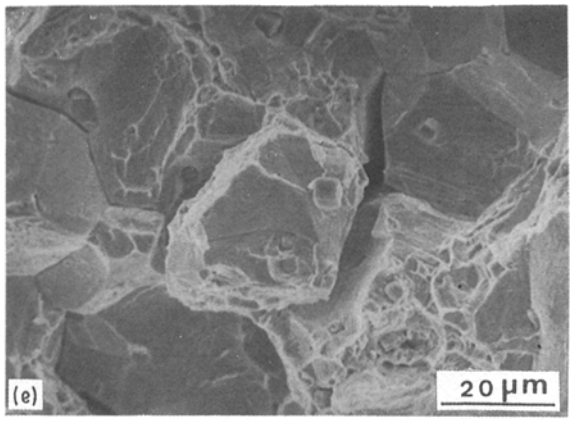


*Figure 7* Variation of the fracture patterns of the carbon (0.06 wt %)-doped $Ni_3(Si, Ti)$ alloys with test temperature. Note that the tests were performed in vacuum. (a) 77 K, (b) room temperature, (c) 673 K, (d) 773 K, (e) 873 K.

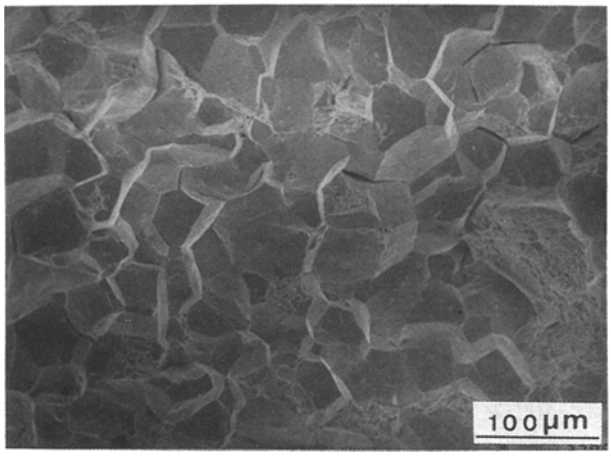


*Figure 8* Fracture pattern of the beryllium (0.1 wt %)-doped $Ni_3(Si, Ti)$ alloy which was tensile tested at room temperature and in vacuum.

in vacuum. This discrepancy became considerable at temperatures above 473 K. Thus, the environmental effect on ductility of the carbon-doped $Ni_3(Si, Ti)$ alloys was the same as that observed in boron-doped $Ni_3(Si, Ti)$ alloys (Figs 9b and 10b) but was very different from that observed in the undoped $Ni_3(Si, Ti)$ alloys (Figs 9c and 10c) [5, 6]. In the undoped $Ni_3(Si, Ti)$ alloys, losses of elongation and UTS values of the specimens tested in air were significant at ambient temperature. It was also shown in this case that as the test temperature increased to about 473 K the ductility values tested in air recovered to the values of the specimens tested in vacuum.

It is concluded from these figures that the environmental embrittlement for the carbon-doped and boron-doped $Ni_3(Si, Ti)$ alloys is not operative at ambient temperatures but is obvious at elevated temperatures, whereas the environmental embrittlement for the undoped $Ni_3(Si, Ti)$ alloys is significant at ambient temperatures but was not found at elevated temperatures.

In the previous section, fractographs of the carbon-doped $Ni_3(Si, Ti)$ alloys tensile tested in vacuum were shown as a function of testing temperature. The description was in terms of the temperature dependence of the fracture patterns. Here, the fractographs of the specimens tensile tested in air are shown in Fig. 11; the fracture surfaces are shown at two different magnifications and also as a function of testing temperature.

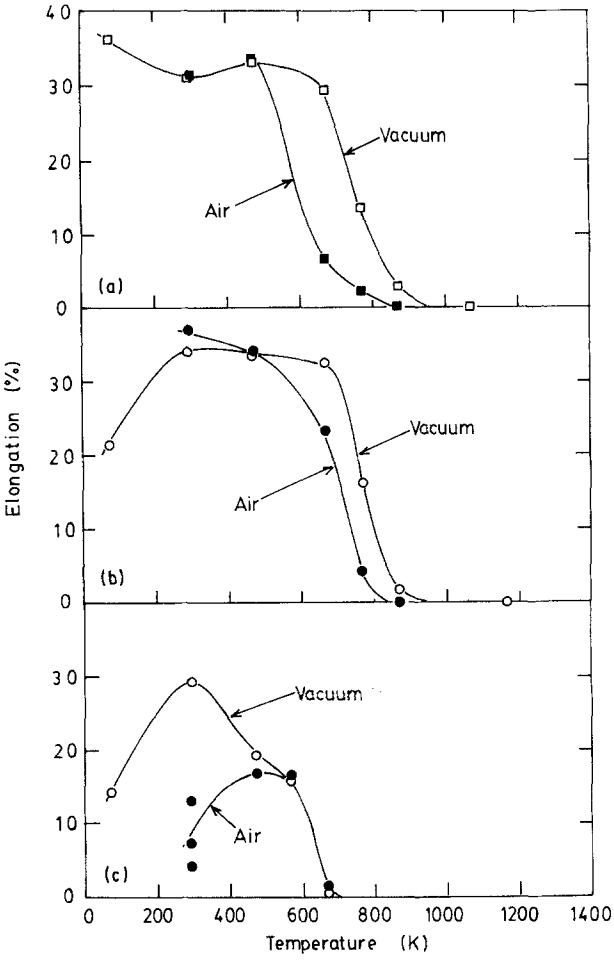


*Figure 9* Variations of elongation of (a) the carbon (0.06 wt %)-doped $Ni_3(Si, Ti)$ alloys, (b) the boron (50 p.p.m.)-doped $Ni_3(Si, Ti)$ alloys and (c) the undoped $Ni_3(Si, Ti)$ alloys with test temperature. The results were compared between two environments: vacuum and air. Note that the data for the boron (50 p.p.m.)-doped and the undoped $Ni_3(Si, Ti)$ alloys were taken from [6].

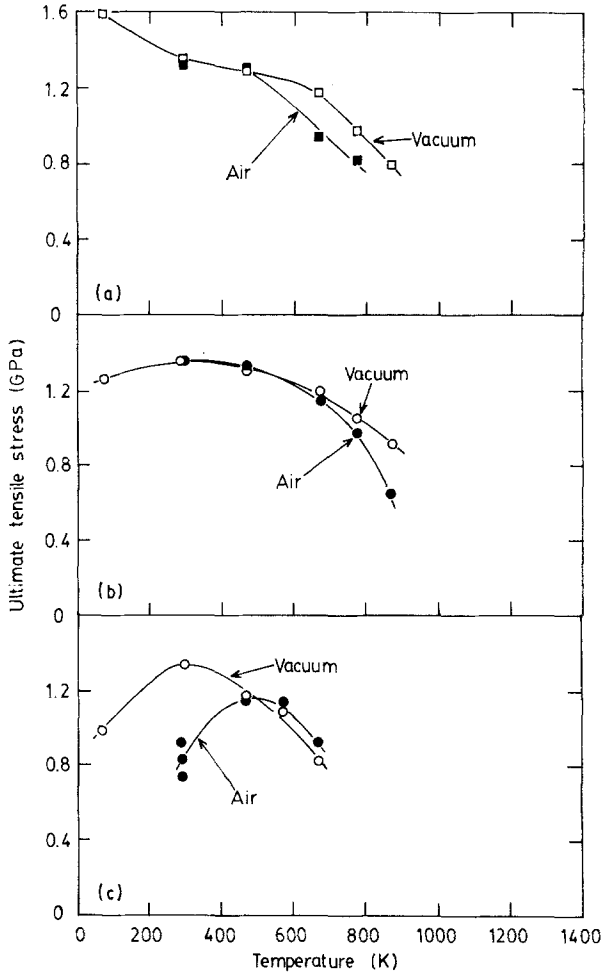


*Figure 10* Variations of UTS of (a) the carbon (0.06 wt %)-doped $Ni_3(Si, Ti)$ alloys, (b) the boron (50 p.p.m.)-doped $Ni_3(Si, Ti)$ alloys and (c) the undoped $Ni_3(Si, Ti)$ alloys with test temperature. The results were compared between two environments: vacuum and air. Note that the data for the boron (50 p.p.m.)-doped and the undoped $Ni_3(Si, Ti)$ alloys were taken from [6].

The fractography of the specimens tensile tested at room temperature showed mostly ductile transgranular fracture patterns and is very homogeneous over the whole cross-section of the specimen. Also, it should be noted that the fracture pattern is quite similar to that tensile-tested in vacuum (cf. Fig. 7). Thus, this result corresponds well with that showing that two specimens tensile-tested in vacuum and air showed almost identical, high values of elongation and UTS.

Very striking fracture patterns were observed in the specimens tensile-tested at 673 and 773 K. In this temperature region, the fractography of the specimens tensile tested in air was very heterogeneous in contrast to the specimens tensile tested in vacuum; the intergranular fracture patterns were preferentially observed in the region near the specimen-free surface and tended to be less dominant on approaching the specimen interior. Also, this surface-affected layer expanded more towards the specimen interior with increasing temperature. Thus, it appears that intergranular fracture observed near the specimen surface was caused by tensile testing in air. Again, this result corresponds well to that for the specimens tensile tested in air, showing lower values of elongation and UTS than those tensile tested in vacuum.

Detailed fractographic observation was performed on the surface-affected zone of the carbon-doped $Ni_3(Si, Ti)$ alloys which were tensile tested in air at high temperatures. However, no microstructures revealing low melting phase particles or new phase particles (perhaps containing elemental oxygen) were identified on the grain-boundary facets in the surface-affected zone.

## 4. Discussion

The behaviour of the carbon atoms in the $Ni_3(Si, Ti)$ alloys was quite similar to the behaviour of the boron atoms [4–6, 8] in terms of (1) lattice parameters, (2) solubility limit, (3) strengthening, (4) ductilization and (5) environmental effects.

1. Both atoms were supposed to behave as interstitial atoms in a perfect lattice and also to segregate into the grain boundaries.
2. They showed very low solubility limits (i.e. of the order of p.p.m.), consequently resulting in the carbide or the boride in the higher contents of both atoms.
3. Neither of the atoms produced any apparent strengthening. However, both atoms may be capable

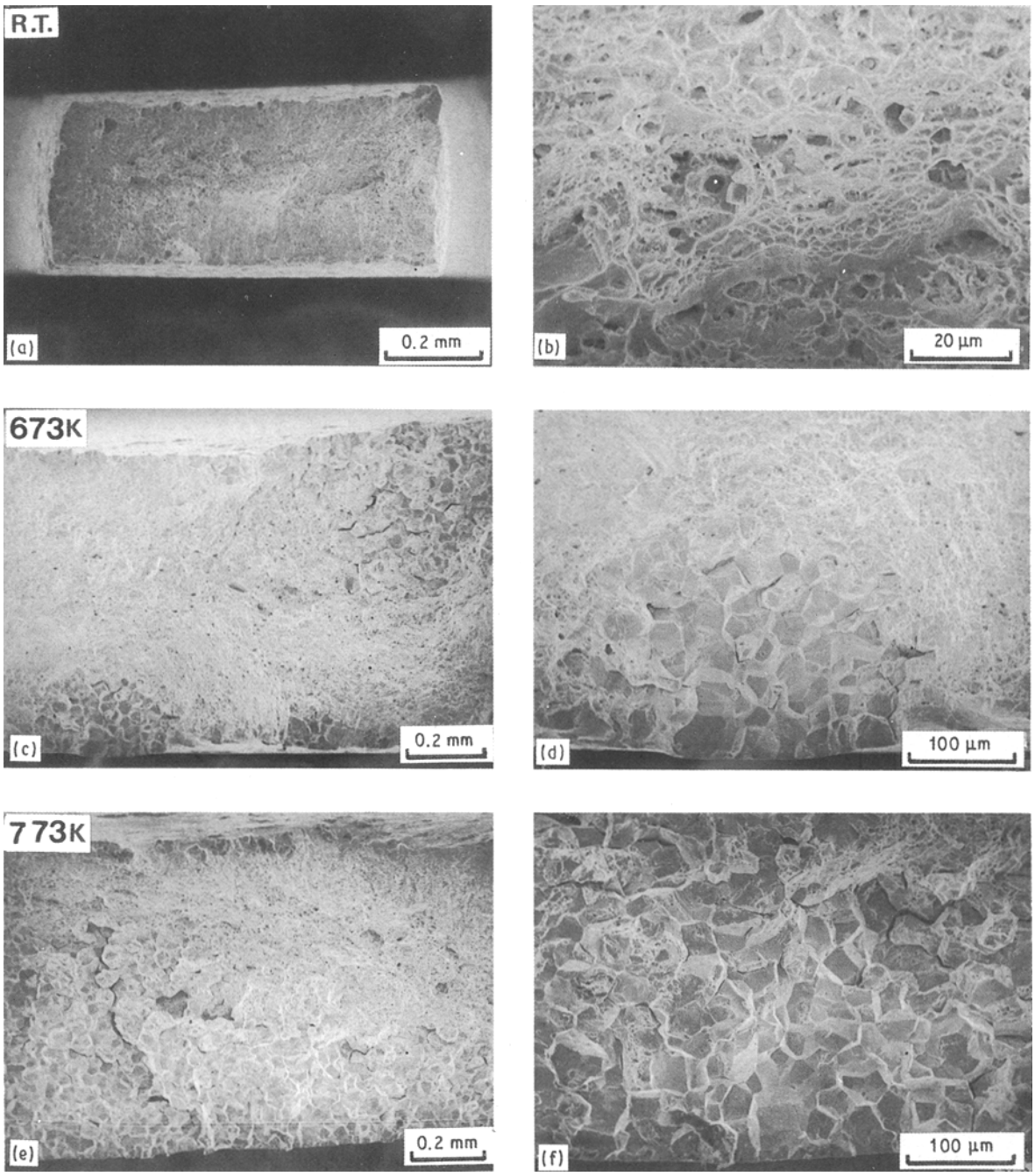


*Figure 11* Variation of the fracture patterns of the carbon (0.06 wt %)-doped $Ni_3(Si, Ti)$ alloys with test temperature. Note that the tests were performed in air. (a, b) Room temperature, (c, d) 673 K, (e, f) 773 K.

of significant strengthening if they were sufficiently soluble as solutes.

4. Both atoms improved the ductilities of elongation and UTS over a wide temperature range.

5. Neither of the atoms showed environmental embrittlement operative at ambient temperatures but they did show environmental embrittlement operative at elevated temperatures.

These results are totally due to the same electronic nature, as understood from the position of two atoms in the Periodic Table.

On the other hand, the behaviour of the beryllium atoms was different from the behaviour of the previous two atoms.

1. Atomic beryllium behaved as a substitutional atom in the perfect lattice.

2. It showed a relatively larger solubility limit.

3. Atomic beryllium produced a moderate strengthening, perhaps due to the size and/or elastic interaction between the beryllium and the constituent atoms.

4. It reduced the ductility.

Higher elongation values were found in the carbon-doped $Ni_3(Si, Ti)$ alloys even containing second-phase particles. In the case of boron-doped $Ni_3Al$ alloy, the formation of the boride caused complete elongation loss [9] whereas in the cases of the beryllium-doped $Ni_3Al$ [10] and the boron-doped $Ni_3(Si, Ti)$ alloys [5, 6], the formation of the second-phase particles did not always reduce the elongation values. Therefore, it must be noted here that a trace amount of free carbon dissolved in the matrix is certainly beneficial to the

ductility of this alloy, through segregation to the grain boundaries and also precipitation of second phases in the grain interior is not so harmful. However, the greatest ductility improvement in the carbon-doped $Ni_3(Si, Ti)$ alloys is expected by doping with a very low level of carbon which was completely soluble. In the $Ni_3Si$ binary alloys, Oliver and White observed a maximum elongation value on doping with 0.015 wt % carbon [1].

Doping with 0.1 wt % beryllium reduced the ductility of the $Ni_3(Si, Ti)$ alloys. However, because Oliver and White have observed a beneficial effect on the elongation by doping with 0.015 wt % beryllium in the binary $Ni_3Si$ alloys [1], an optimal content of beryllium doping may also be found in the $Ni_3(Si, Ti)$ alloys.

For the carbon-doped $Ni_3(Si, Ti)$ alloys, it was clearly demonstrated that no environmental effect operative at low temperatures was found, whereas an environmental effect operative at high temperatures was evident. It has been suggested that the environmental effect at low temperatures is associated with hydrogen embrittlement to [3, 11, 12], while the environmental effect at high temperatures is associated with oxygen embrittlement [13]. Thus, both environmental embrittlements are attributed to the gaseous species composed of air. Thus, the effect of carbon doping on these phenomena could be interpreted by understanding the interaction between hydrogen and carbon or the interaction between oxygen and carbon in the corresponding temperature regime.

The undoped $Ni_3(Si, Ti)$ alloys actually suffered from hydrogen-related embrittlement [6]. This kind of environmental embrittlement has been widely observed for a number of $L1_2$-type ordered alloys [11–13]. A micro-mechanism associated with this phenomenon was proposed [14, 15]; a dynamic and atomistic mechanism by which the cohesive strength of a grain boundary [14] and the associated plastic flow around a micro-crack were affected by the hydrogen [15], has been suggested. This kind of embrittlement disappears at high temperatures and therefore is dominantly operative only at low temperatures. However, the results observed in the carbon-doped $Ni_3(Si, Ti)$ alloys clearly indicate that the carbon atoms suppressed the environmental embrittlement in air. Therefore, it is suggested that the carbon atoms competing with the hydrogen atoms, for site occupation or for its effectiveness at grain boundaries, have the effect of suppressing hydrogen embrittlement. As already described in the previous section, a similar action has been observed for the boron atoms in the $Ni_3(Si, Ti)$ alloys [6].

The undoped $Ni_3(Si, Ti)$ alloys did not suffer from the embrittlement due to the oxygen. However, the carbon-doped $Ni_3(Si, Ti)$ alloys showed this kind of environmental embrittlement. A similar embrittlement was observed in boron-doped $Ni_3(Si, Ti)$ alloys [6] and also in boron-doped $Ni_3Al$-based alloys [14]. It was suggested that this embrittlement was due to a dynamic effect simultaneously involving localized stress concentrations at grain boundaries and gaseous oxygen at elevated temperatures. The process of this oxygen embrittlement has been considered to consist of some general steps [13].

One possible explanation of the oxygen embrittlement observed in this work is that the low melting (eutectic) phase consisting of oxygen and carbon (and/or constituent elements of nickel, silicon and titanium) may be formed during dynamic loading, resulting in the easier separation of grain boundaries. Indeed, the dendritic phases were observed at grain boundaries near the specimen surface of the boron-doped $Ni_3(Si, Ti)$ alloys and may play a role in this embrittlement [6]. However, in the present case, detailed fractographic observation indicated that no second phases were formed during the deformation. Alternatively, a second possibility is suggested; the grain-boundary cohesion associated with the bonds among the constituent atoms is strongly reduced by the coexistence of oxygen with carbon, and the bond breakings occur dynamically. Although the latter explanation is likely, more detailed observation is required to understand the phenomenon observed here.

## 5. Conclusions

The $Ni_3(Si, Ti)$ alloys doped with carbon (0.03 wt % and 0.06 wt %) and beryllium (0.1 wt %) were tensile tested in vacuum and air over a wide range of test temperatures, and then compared with the results for the undoped and boron-doped $Ni_3(Si, Ti)$ alloys previously reported [5, 6]. The following results were obtained.

1. The solubility limits of carbon and beryllium were shown to be below 0.03 wt % and above 0.1 wt %, respectively. The carbon-doped $Ni_3(Si, Ti)$ alloys contained second-phase particles while the beryllium-doped $Ni_3(Si, Ti)$ alloys consisted of a single phase with $L1_2$ structure.

2. The yield stresses of the carbon-doped $Ni_3(Si, Ti)$ alloys were almost identical to the undoped $Ni_3(Si, Ti)$ alloys while those of the beryllium-doped $Ni_3(Si, Ti)$ alloys were slightly higher than the undoped $Ni_3(Si, Ti)$ alloys.

3. Doping with carbon in the $Ni_3(Si, Ti)$ alloys enhanced the elongation and UTS values, whereas doping with beryllium in the $Ni_3(Si, Ti)$ alloys reduced these values over the entire test temperature range.

4. The fracture patterns were primarily associated with the degree of elongation (or UTS) itself. As the elongation (or UTS) value increased, the fracture pattern changed from intergranular to transgranular.

5. No environmental effect on the ductility of the carbon-doped $Ni_3(Si, Ti)$ alloys was found at ambient temperatures, but a significant effect was seen at elevated temperatures. The elongation and UTS values were reduced at high temperatures when these alloys were tensile tested in air.

6. The carbon-doped $Ni_3(Si, Ti)$ alloys tensile tested in air and at high temperatures showed very heterogeneous fracture patterns: almost intergranular near the specimen surface and less intergranular in the specimen interior.

7. The environmental embrittlement observed at high temperatures, was suggested to be caused by the

penetration of free oxygen into the grain boundaries causing a loss of ductility in the carbon-doped $Ni_3(Si, Ti)$ alloys.

## Acknowledgements

This research was partly supported by the Grant-in-Aid for Scientific Research on Priority Areas, New Functionality Materials-Design, Preparation and Control, The Ministry of Education, Science and Culture. The authors thank Professor Emeritus O. Izumi, Tohoku University, for his encouragement.

## References

1. W. C. OLIVER and C. L. WHITE, in "Proceedings of the MRS Symposium on High-Temperature Ordered Intermetallic Alloys II", edited by N. S. Stoloff, C. C. Koch, C. T. Liu and O. Izumi, Vol. 81 (1987) pp. 241–6.
2. O. IZUMI and T. TAKASUGI, *ibid.*, Vol. 81, pp. 173–82.
3. *Idem., J. Mater. Res.* **3** (1988) 426.
4. T. TAKASUGI, M. NAGASHIMA and O. IZUMI, *Acta Metall. Mater.* **38** (1990) 747–55.
5. T. TAKASUGI, O. IZUMI and M. YOSHIDA, *J. Mater. Sci.*
6. T. TAKASUGI, H. SUENAGA and O. IZUMI, *ibid.*
7. T. TAKASUGI and M. YOSHIDA, *ibid.*
8. T. TAKASUGI, D. SHINDO, O. IZUMI and M. HIRABAYASHI, *Acta Metall. Mater.* **38** (1990) 739–45.
9. C. T. LIU, C. L. WHITE and J. A. HORTON, *Acta Metall.* **33** (1985) 213.
10. T. TAKASUGI, N. MASAHASHI and O. IZUMI, *Scripta Metall.* **20** (1986) 1317.
11. C. T. LIU, in "Proceedings of the MRS Symposium on High-Temperature Ordered Intermetallic Alloys II", edited by N. S. Stoloff, C. C. Koch, C. T. Liu and O. Izumi, Vol. 81 (1987) pp. 355–67.
12. N. S. STOLOFF, *J. Metals* **40** (12) (1988) 18.
13. C. T. LIU and C. L. WHITE, *Acta Metall.* **35** (1987) 643.
14. T. TAKASUGI and O. IZUMI, *ibid.* **34** (1986) 607.
15. Y. LIU, T. TAKASUGI, O. IZUMI and T. YAMADA, *ibid.* **37** (1989) 507.

*Received 29 May*
*and accepted 26 June 1990*